Electrochemical Detection of Dopamine in the Presence of Ascorbic Acid Using GS@Mn$_3$O$_4$/Nafion Film Modified Electrode at a Low Working Potential

*Guowen He[1,2, *], Dan Wu[1,2], Guqing Xiao[1,2]*

[1]College of Chemical and Enviromental Engineering, Hunan City University, Yiyang, 413000, PR China
[2] Institute of Polymer Materials and Engineering, Hunan City University, Yiyang, 413000, PR China
[*]E-mail: heguowen2014@163.com

Graphene sheets (GS)@manganic manganous oxide (Mn$_3$O$_4$) nanocomposites were prepared via a simple solvothermal process. GS@Mn$_3$O$_4$/nafion (Nf) film modified glassy carbon electrode (GCE) was fabricated and applied for the detection of dopamine (DA) without the interference of ascorbic acid (AA) at the low working potential. The prepared nanocomposites (GS@Mn$_3$O$_4$) were characterized by X-ray diffraction (XRD) and fourier transform infrared spectroscopy (FT-IR), and the morphology of different electrodes was characterized by scanning electron microscopy (SEM). The electrochemical properties of the modified electrode (GCE│GS@Mn$_3$O$_4$/Nf) were investigated by electrochemical impedance spectroscopy (EIS), cyclic voltammetry (CV) and current-time method (i-t curve). Under the optimized experimental conditions, the i-t curve showed a linear dependence on DA concentrations ranging from 1.0×10^{-6} to 1.3×10^{-3} M (*R*=0.9985) with a detection limit of 8.0×10^{-8} M (S/N=3). The proposed method was used to detect DA in real pharmaceutical samples using the standard addition method without additional sample pre-treatment with satisfactory results, which showed great promise for screen-determination of DA in real samples.

Keywords: GS@   Mn$_3$O$_4$; Dopamine; Low working potential

1. INTRODUCTION

Dopamine (DA) is one of the most important catecholamines, which plays an important role in the function of several physiological systems [1]. Hence, the sensitive determination of DA is an important issue for molecular disease diagnosis and therapeutic efficacy evaluation [2].

Various analytical methods including fluorometry [3, 4], chromatography [5], electrochemiluminescence [6] and electrochemical technique (ET) [7-9] have been reported for DA detection. Among those methods, ET is considered as a useful approach owing to its high sensitivity, cost-effectiveness, ease of operation and capability of in situ detection. From the molecular structure, it is apparent that DA is an easily oxidizable compound. Thus, ET based on its anodic oxidation has attracted growing interests [10, 11]. Unfortunately, DA often encounter interferences from other common co-existing protocols such as ascorbic acid (AA), which is readily oxidized on the working electrode. Furthermore, AA and DA are oxidized at nearly the same working potential. Hence an overlapping voltammetric response for the oxidation of a mixture of AA and DA is usually obtained in the bare electrode [12, 13]. Therefore, the selective detection of DA is other major goal in this research field. As such, bare electrodes modified with various materials and approaches have been developed to solve these problems, in order to decrease the overpotential, enrich the substance and promote the electron transfer rate, including sodium dodecyl sulfate-modified carbon paste electrodes [14], MnOOH nanobelt modified electrode [15], cibacron blue/poly-1,5-diaminonaphthalene composite film [16], carbon nanotubes-ionic liquid gel modified electrode [17] and MnO_2 nanowires/chitosan modified gold electrode [18]. Although all the mentioned materials and approaches showed good signals and performance, novel materials, especially novel nanocomposites are still needed to develop highly selective and sensitive DA sensing platform. For the nanocomposites have some synergistic effects (eg. high surface area, increased electron transport, low detection limit and better signal-to-noise ratio) compared with single nanoparticle [19-21].

Graphene sheets (GS) has been considered as a ''rising-star'' and drawn considerable attention for its fascinating properties and wide applications [22]. In more recently, GS-based nanocomposites has been developed as an advanced nano-material for constructing various electrochemical DA sensors [22-25]. Manganic manganous oxide (Mn_3O_4) is a very useful transition metal oxide, has been widely used in various fields such as lithium-ion batteries [26], supercapacitors [27, 28] and catalyst [29], attributing to its low toxicity, low cost, good electrochemical activity and large abundance. However, up to date, there is no report on the electroanalysis performance of Mn_3O_4 modified electrode towards DA determination. Nafion (Nf) is a large biopolymer and has been applied to disperse different nanomaterials on the surface of solid substrates. The interference of AA can be partly avoided by coating the electrode surface with Nf film, but the use of Nf alone obviously can not solve the sensitivity [30].

Herein, we reported the fabrication of an electrochemical sensor based on GS@Mn_3O_4 nanocomposites and Nf film modified glassy carbon electrode (GCE) for selective and sensitive amperometric detection of DA at the low working potential (+0.02 V *vs*. SCE) for the first time. The proposed modified electrode (GCE│GS@Mn_3O_4/Nf) showed significantly improved selectivity attributed to low working potential. Meanwhile, the modified electrode exhibited superior electrochemical activity and noticeably enhanced the peak current for DA determination. Finally, the modified electrode has been successfully applied to analyze DA in real injection solution samples with satisfactory results.

2. EXPERIMENTAL

2.1. Reagents

Graphite powder was purchased from green battery material limited company (Changsha, China). Nf solution, $Mn(Ac)_2 \cdot 4H_2O$ and other chemicals were of analytical-reagent grade and used without further purification were obtained from sinopharm medicine holding co., ltd (Shanghai, China). L-Ascorbic acid (AA) and Dopamine hydrochloride (DA) were obtained from Sigma-Aldrich and used as received without further purification. The 0.1 M phosphate buffer solution (PBS) at various pH values was prepared by mixing the stock solutions of 0.1 M Na_2HPO_4 and 0.1 M NaH_2PO_4 with different proportion. Doubly distilled water (18.2 MΩ) was used throughout.

2.2. Apparatus

Electrochemical measurements were performed on a CHI 660D electrochemical workstation (CHI Instruments, Shanghai, China) using a classical three electrode configuration of a GS@Mn$_3$O$_4$/Nf modified GCE (3 mm diameter) as the working electrode, a platinum wire as the auxiliary electrode and a saturated calomel electrode (SCE) as the reference electrode. The morphology of different electrodes was characterized by the scanning electron microscopy (SEM, Hitachi S-4800N). The fourier transform infrared (FT-IR) spectroscopy of the products was recorded with a KBr pellet on the IR prestige-21 (Shimadzu) spectrometer. The x-ray powder diffractometer (XRD, Rigaku Ultima IV, Cu Kα radiation) was used to determine the phase purity and crystallization degree of nanoparticles.

2.3. Preparation of the GS@Mn$_3$O$_4$ nanocomposites

In the first step, graphite oxide was obtained from natural graphite by a modified Hummers method [31]. Then, exfoliation of graphite oxide to graphene oxide (GO) was achieved by ultrasonication of the dispersion for 30 min. The 0.5 mg/mL homogeneous GO suspension was prepared by ultrasonication of 13.5 mg GO in 27 mL 9:1 ethanol/H_2O mixed solvent for 3 h. Then 2.7 mM of $Mn(AC)_2 \cdot 4H_2O$ was dissolved in the GO suspension by stirring. Finally, the resulting solution was transferred into a 30 mL Teflonlined stainless steel autoclave, and treated at 180 ℃ for 10 h. After the reaction, the autoclave was allowed to cool to room temperature. The precipitate was washed with alcohol and water several times, then freeze dried for 24 h, and the final product was denoted as GS@Mn$_3$O$_4$ nanocomposites.

2.4. Fabrication of the GS-Mn$_3$O$_4$/Nf modified GCE

The GS@Mn$_3$O$_4$/Nf suspension was prepared by dispersing GS@Mn$_3$O$_4$ nanocomposites (50 mg) in 100 mL of Nf solution (0.2 *wt%*) under vigorously ultrasonication for about 20 min. Prior to the modification, the bare GCE was polished with emery paper and chamois leather containing 0.3 and 0.05 μm Al_2O_3 slurry, respectively, thoroughly rinsed with water, and sonicated in ethanol, HNO_3 and

distilled water in turn. After being cleaned, 5.0 μL of the resulting GS@Mn$_3$O$_4$/Nf dispersion was dropped onto the surface of the GCE and dried under the infrared lamp till dry (labeled as GCE│GS@Mn$_3$O$_4$/Nf). After modification, the modified electrode was thoroughly rinsed with water and kept at room temperature for further use. For comparison, a Nf solution (0.2 *wt%*) without GS@Mn$_3$O$_4$ nanocomposites was deposited onto other GCE to fabricate the Nf film modified GCE (labeled as GCE│Nf).

3. RESULTS AND DISCUSSION

3.1. Characterization of the synthesised GS@Mn$_3$O$_4$ nanocomposites

The crystal structures of GO, GS and GS@Mn$_3$O$_4$ were determined by XRD. In Fig.1-a, the typical diffraction peak (002) of graphite shifts to 2θ=10.6°, which is ascribed to the introduction of various oxygenic functional groups (carboxyl, hydroxyl, epoxy and carbonyl) attached on both edges and sides of the graphite sheets [32]. The XRD of GS was shown in Fig.1-b. Due to the partial removal of the oxygen-containing functional groups during reduction process, the weak diffraction peak of GS shifts to 2θ=23° and is in good agreement with graphite. That means the partially reduction of GO to GS and restacked into a disordered crystalline structure [33]. As seen in Fig.1-c, the peak at 23° is indexed to the graphitic plane (002) of GS, all other peaks of GS@Mn$_3$O$_4$ nanocomposites can be indexed to Mn$_3$O$_4$ based on their good agreement with JCPDS card (No. 24-0734). The sharpness of the diffraction peaks also indicates the high crystallinity of Mn$_3$O$_4$ in GS@Mn$_3$O$_4$ nanocomposites [27].

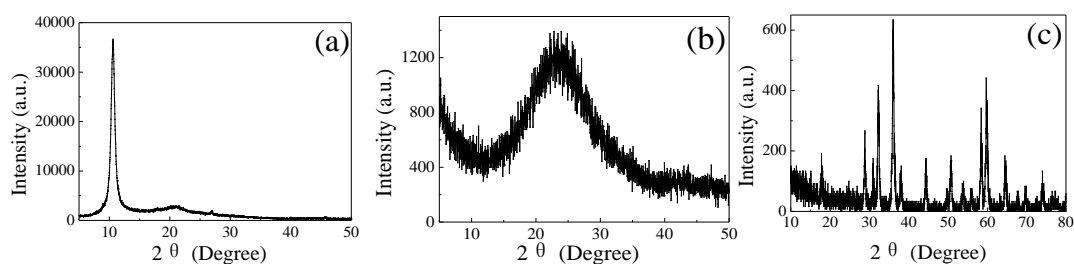**Figure 1.** XRD patterns of the GO (a), GS (b) and GS@Mn$_3$O$_4$ (c).

The FT-IR spectroscopy of GO and GS@Mn$_3$O$_4$ nanocomposites are shown in Fig.2. In the FT-IR of GO (Fig.2-a), stretches of alkoxy, epoxy C-O, carboxyl C-O, aromatic C=C, C=O and O-H can be found at 1060, 1230, 1410, 1620, 1730 and 3400 cm^{-1}, respectively, in good agreement with previous report [26]. The FT-IR of GS@Mn$_3$O$_4$ nanocomposites (Fig.2-b) shows that peaks for oxygen function groups are significantly weakened or entirely removed. Two peaks at 1230 and 1620 cm^{-1} can be assigned to the aromatic C-O stretch and the C=C stretch, separately. The absorption at 3400 cm^{-1} indicates the presence of hydroxide group. In addition, two broad absorption bands can be found at 618 and 515 cm^{-1}, which are associated with the coupling mode between Mn-O stretching modes of

tetrahedral and octahedral sites. The peak at 413 cm^{-1} is due to the bandstretching mode of the octahedral sites [26]. Thus, the FT-IR results further confirm the formation of GS@Mn$_3$O$_4$ nanocomposites.

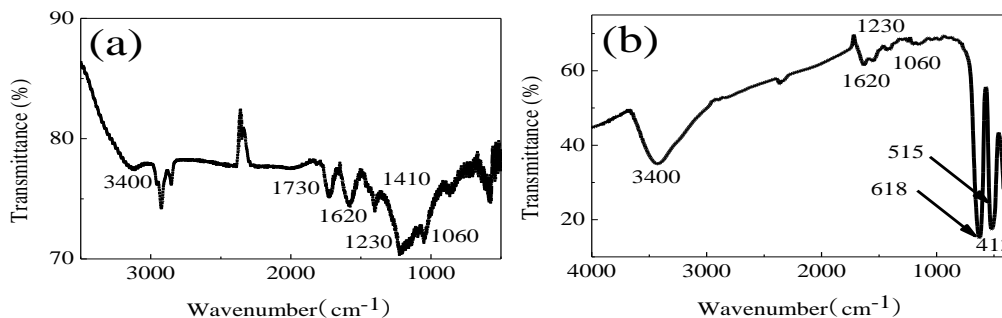**Figure 2.** FT-IR spectroscopy of the GO (a) and GS@Mn$_3$O$_4$ (b).

Fig.3-a appears the smooth surface morphology of the GCE. While the Nf solution was deposited onto the GCE to fabricate the GCE│Nf electrode, uniform Nf film was formed on the GCE (Fig.3-b). As indicated in the magnified SEM image, the surface of GCE│GS@Mn$_3$O$_4$/Nf electrode exhibits a few thin wrinkles of GS and Mn$_3$O$_4$ nanoparticles are densely dispersed on the GS (Fig.3-c). The diameter of individual Mn$_3$O$_4$ nanoparticles is about 50 nm, which is advantageous to enhance the sensitivity and selectivity for electrochemical detection of DA.
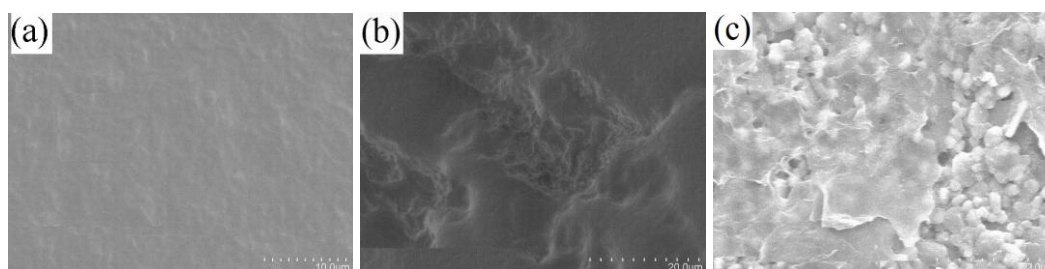
Figure 3. SEM images of the GCE (a), GCE│Nf (b) and GCE│GS@Mn$_3$O$_4$/Nf (c) electrodes.

3.2. Electrochemical behaviors of the different electrodes

Cyclic voltammetry (CV) method was used to investigate the electrochemical behaviors of different electrodes. Fig. 4-A depicts the cyclic voltammetries (CVs) for 5.0 mM K$_3$[Fe(CN)$_6$] at different electrodes. The redox current at the GCE (curve a) is smaller than that at the GCE│GS@Mn$_3$O$_4$/Nf electrode (curve b), but somewhat larger than that at the GCE│Nf electrode (curve c). The result illustrates that the Nf film on the electrode would reduce the redox current and the GS@Mn$_3$O$_4$ nanocomposites to current amplification is higher than the Nf film to current reduction [34]. The electrochemical impedance spectroscopy (EIS) method was used to assess the capability of electron transfer of different electrodes. The Nyquist plots of different electrodes in 10.0 mM

$[Fe(CN)_6]^{3-/4-}$ (1:1) solution were shown in Fig.4-B. The linear part at the lower frequency region and the distinct semicircular at the higher frequency region correspond to the diffusion limited process of the electrochemical reaction and the electron transfer, respectively. The inset of Fig.4-B shows a standard Randle's equivalent circuit model, including a charge transfer resistance (Rct), warburgh impedance (Zw), constant phase element (Q) and the uncompensated solution resistance (Rs) were used to fit the impedance data. Rct, which is equivalent to the diameter of the semicircular, could be used to express the conduction capacity of the electrode indirectly. The Rct values of the GCE (a), GCE│Nf (b) and GCE│GS@Mn$_3$O$_4$/Nf (c) electrodes are found to be 120, 2980 and 1450 Ω, respectively from the Nyquist plots, indicating that the conductivity of the GCE│GS@Mn$_3$O$_4$/Nf electrode is better than that of the GCE│Nf electrode.
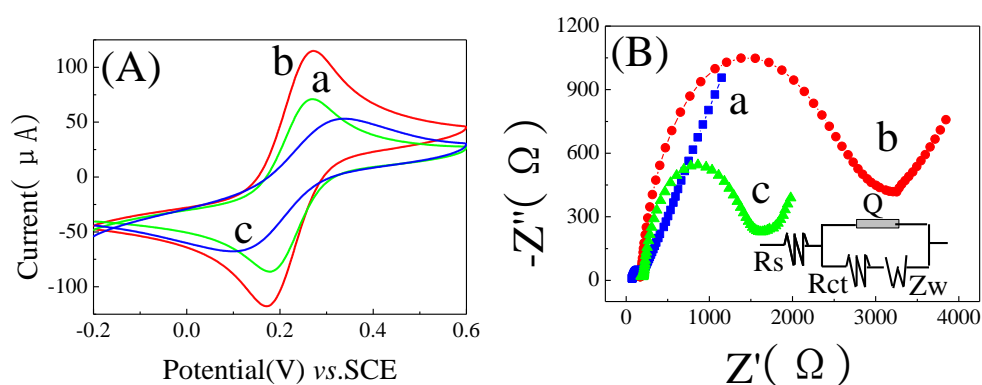

Figure 4. CVs (A) and EIS (B) of the GCE (a), GCE│Nf (b) and GCE│GS@Mn$_3$O$_4$/Nf (c) electrodes in 0.1 M KCl solution containing 5.0 mM K$_3$[Fe(CN)$_6$] and 10.0 mM [Fe(CN)$_6$]$^{3-/4-}$(1:1).

3.3. Electrochemical behaviors of DA at different electrodes

The electrochemical responses of different electrodes to DA were investigated by cycling the potential between + 0.8 and - 0.2 V at 0.1 V/s as depicted in Fig. 5. The GCE presents a pair of irreversible redox peak of DA (curve a). However, the response of the Nf film modified GCE (GCE│Nf) is lower than GCE (curve b), which can be interpreted as that the Nf film could slow down the diffusion of the reactant to the electrode surface. In contrast, the GCE│GS@Mn$_3$O$_4$/Nf electrode shows a well-defined cathodic peak at about + 0.05 V for DA (curve c). It may deduce that the electron transfer is remarkably enhanced by GS@Mn$_3$O$_4$ nanocomposites which distribute uniformly within the Nf film and can serve as the electron mediator. The reduction peak is more negatively shifted as compared to that at both the GCE and GCE│Nf electrodes, implying that the immobilized GS@Mn$_3$O$_4$ nanocomposites may play a role in the electro-reduction of DA. The low reduction peak potential of DA at + 0.05 V on the GCE│GS@Mn$_3$O$_4$/Nf electrode is favorable for selective detection of DA, bacause this could be reduce interference from other electro-active species. Additionally, it is found that the reduction peak current at the GCE│GS@Mn$_3$O$_4$/Nf electrode increases with the concentration of DA increases (curve d), indicating its potential application for DA analysis. The CVs of the GCE│GS@Mn$_3$O$_4$/Nf electrode in 0.1 M PBS containing 0.1 mM DA at various scan rates (*v*, 0.01-

0.1 V/s) were also investigated. Both the oxidation and reduction currents increase with the *v* and there is a good linear relationship between current and *v*, indicating that the electrochemical reaction of DA on the modified electrode should be controlled by a typical adsorption process [35].
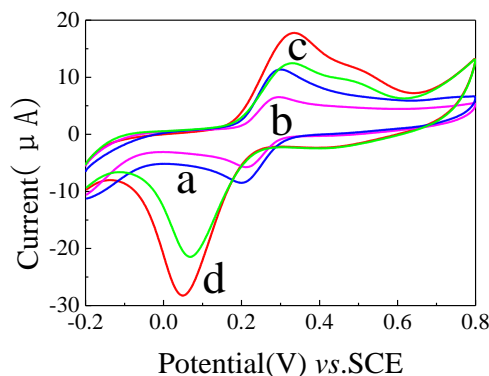

Figure 5. CVs of the GCE (a), GCE│Nf (b) and GCE│GS@Mn$_3$O$_4$/Nf (c) electrodes in 0.1 M PBS containing 0.1 mM DA and GCE│GS@Mn$_3$O$_4$/Nf electrode in 0.1 M PBS containing 0.2 mM DA (d).

3.4. Optimization conditions of the electrochemical sensor

The effects of some electrolytes, such as 0.1 M PBS, NH$_3$·H$_2$O-NH$_4$Cl and NaAc-HAc on stripping peak currents of 0.1 mM DA was studied. The best shape of peak, the lowest background current and the largest stripping peak current were obtained in 0.1 M PBS. The influence of pH on the determination of DA was also investigated. At first, the peak currents of 0.1 M DA increase gradually as the pH from 4.0 to 4.5, achieve a maximum value at about pH 4.5 and then continuous increase of pH led to a decrease of the peak current. Thus, 0.1 M PBS (pH 4.5) was choosn as the optimal supporting electrolyte, which in agreement with the previous report [36].

The effect of the GS@Mn$_3$O$_4$/Nf suspension loading on the GCE on the performance of the GCE│GS@Mn$_3$O$_4$/Nf electrode to 0.1 mM DA was investigated. The response currents to 0.1 mM DA increase when the added volume of GS@Mn$_3$O$_4$/Nf suspension increase from 3.0 to 5.0 μL, then gradually decreased after exceeded to 5.0 μL. The results infers that appropriate amount of GS@Mn$_3$O$_4$/Nf suspension is favorable to enhance the sensitivity of the modified electrode. However, excess amount would make the modified film too thick and block the electrons transfer [37]. Therefore, 5.0 μL of GS@Mn$_3$O$_4$/Nf suspension was selected as the amount of modification.

The quantity of GS@Mn$_3$O$_4$ nanocomposites in the Nf solution is a critical parameter for electrochemical performance of the modified electrode. The response currents to 0.1 mM DA increase with the increase in the amount of GS@Mn$_3$O$_4$ nanocomposites in the Nf solution until 0.5 mg/mL. Higher quantity of GS@Mn$_3$O$_4$ nanocomposites broadening of voltammogram and does not improve the response current. So, the optimal conditions for fabrication of the GCE│GS@Mn$_3$O$_4$/Nf electrode is 5.0 μL of GS@Mn$_3$O$_4$ suspension (0.5 mg/mL) in the Nf solution.

The effect of the operating potential on the amperometric response of the GCE│GS@Mn$_3$O$_4$/Nf electrode to 0.1 mM DA was also studied. The maximum response current was obtained at + 0.02 V.

3.5. The detection of DA on the GCE│GS@Mn$_3$O$_4$/Nf electrode

Under the optimal experimental conditions, the typical amperometric response of the GCE│GS@Mn$_3$O$_4$/Nf electrode with successive injection of DA in 0.1 M PBS at +0.02 V was given in Fig.6-A. The modified electrode responded rapidly when DA was added and reached a steady state (95% of the maximum value) within 3 s (curve 1), indicating a fast diffusion of the substrate in the hybrid film modified on the electrode and the high sensitivity of the modified electrode. Fig.6-B shows the response current at the GCE│GS@Mn$_3$O$_4$/Nf electrode is linearly related to the concentration of DA in the range from 1.0×10^{-6} to 1.3×10^{-3} M with the linearization equations i (10^{-8} A)= 4.2201 + 0.5294 C_{DA} (C:μM) (R=0.9985). The detection limit was estimated to be 8.0×10^{-8} M based on signal-noise ratio equal to 3 (S/N=3). For comparison, similar experiments were conducted both on GCE│Nf (curve 2 in Fig.6-A) and GCE electrodes (curve 3 in Fig. 6-A) electrodes. No distinct response current to DA is observed in both cases. These results suggest that GS@Mn$_3$O$_4$ nanocomposites play a crucial role in enhancing the current of DA at the surface of the modified electrode.
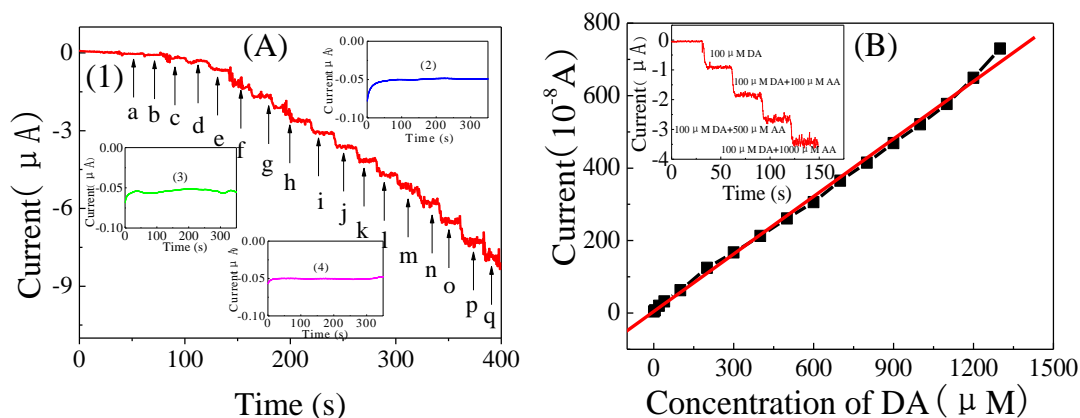

Figure 6. (A) Typical i-t response of the GCE│GS@Mn$_3$O$_4$/Nf (1), GCE│Nf (2) and GCE (3) electrodes upon successive addition of various concentrations of DA: (a) 1.0, (b) 4.0, (c) 15.0, (d) 20.0, (e) 60.0, (f)-(q)100.0 μM and (1) electrode upon successive injection of different concentrations of AA from 1.0 μM to 1.0 mM at + 0.02 V in 0.1 M PBS (4). (B) The linear calibration curve in the DA range 1.0-1300.0 μM. The inset of (B) shows the current response of the (1) electrode to successive injection of 100.0 μM DA with different concertration of AA.

As is known, AA is one of the major interfering species in the electrochemical detection of DA in real samples. Our proposed GCE│GS@Mn$_3$O$_4$/Nf electrode does not show obvious response to AA (curve 4 in Fig.6-A). The inset of Fig.6-B displays the amperometric response of the GCE│GS@Mn$_3$O$_4$/Nf electrode to DA in the presence of AA and negligible interference from AA is observed. This is because that the determination of DA on the GCE│GS@Mn$_3$O$_4$/Nf electrode at +

0.02 V is immune to AA interference and thus overcomes this common problem in real sample DA analysis.

The analytical performance for the electrochemical detection of DA on different modified electrodes were summarized in Table 1. It can be seen that the GCE│GS@Mn$_3$O$_4$/Nf electrode exhibited broader detection range and lower detection limit. It may be due to the good electrochemical activities and high surface-to-volume ratio of GS@Mn$_3$O$_4$ nanocomposites with a lot of electroactive sites and large surface area for DA to react and absorb. Therefore, the GCE│GS@Mn$_3$O$_4$/Nf electrode could be used for the preparation of a DA electrochemical sensor.

Table 1. Comparison of different DA electrochemical sensors.

Electrodes		Method	Linear range (μM)	Detection limit (μM)	References
GCE │	MnOOH	DPV	1.2-200	0.1	15
GCE │	F3GA-PDAN	i-t	5.0-100	0.1	16
GCE │	GS-AuNPs	DPV	5-1000	1.86	38
GE │	SWCNT/Fe$_2$O$_3$	SWV	3.2-31.8	0.36	39
GCE │	GS@Mn$_3$O$_4$/Nf	i-t	1.0-1300	0.08	This work

3.6. Reproducibility, stability and selectivity of the GCE│GS@Mn$_3$O$_4$/Nf electrode

Reproducibility, stability and selectivity are three important characteristics for the modified electrode, which should be investigated.

The reproducibility of the modified electrode was valued at a DA concentration of 1.0 mM with the same GCE│GS@Mn$_3$O$_4$/Nf electrode. The relative standard deviation (*RSD*) was found to be 2.0% for five repeat measurements. The electrode-to-electrode reproducibility was determined in the presence of same concentration DA with five GCE│GS@Mn$_3$O$_4$/Nf electrodes fabricated in the same way and it showed an acceptable reproducibility with *RSD* of 3.8%.

The stability of the GCE│GS@Mn$_3$O$_4$/Nf electrode was also examined by assessing its amperometric response to 1.0 mM DA during storage in ambient conditions over one month. It was found that the proposed electrochemical sensor could retain 90.2% of its initial response current after one month storage, indicating its good long-term stability.

The selectivity of the electrochemical sensor was examined in presence of 1.0 mM DA when the relative error less than ± 5%. The addition of 10-fold concentration of uric acid, glutamic acid, glycine, lysine and tryptophane, 50-fold concentration of glucose, sodium chloride, acetaminophen and calcium chloride did not cause observable interference, indicating that these common interferents do not cause observable interference.

3.7. Analysis of real sample

In order to test the validity of this method, the GCE│GS@Mn$_3$O$_4$/Nf electrode was applied for determination of DA contents in real samples. Before experiments, 1.0 mL DA injection solution were

directly diluted 100 times with 0.1 M PBS electrolyte and without any other pretreatment. Recovery tests was used to examine the reliability and accuracy of this method. The concentration of DA in the injection solution was found to be 52.2 ± 0.8 mM (n=5) and the recoveries was 102.3%, 99.6% and 103.4%, respectively. The results are in good agreement with the labeled value (52.7 mM) and summarized in Tab.2, confirming that the GCE│GS@Mn_3O_4/Nf electrode is feasible to determine the DA concentration in real samples.

Table 2. Determination of DA in injection solution (*n*=5, mM)

Sample	Concentration	This method	Added	Found	Recovery/%	RSD/%
1	52.7	52.2	100.0	154.5	102.3	4.73
2	52.7	53.0	100.0	152.6	99.6	3.65
3	52.7	51.4	100.0	154.8	103.4	2.48

4. CONCLUSIONS

In summary, an electrochemical sensor based on GS@Mn_3O_4 nanocomposites/Nf film modified GCE was successfully fabricated for selective and sensitive amperometric detection of DA at a low working potential. The proposed modified electrode (GCE│GS@Mn_3O_4/Nf) showed significantly improved selectivity due to being modified with nanocomposites, which could amplify the response current and decrease the working potential. It has been successfully applied to analyze DA in real DA injection solution samples with good accuracy and recovery. It may open up a new approach to explore GS@Mn_3O_4-based composite materials for food or drug residues analysis.

References

1. M. Moreno, A.S. Arribas, E. Bermejo, M. Chicharro, A. Zapardiel, M.C. Rodriguez, Y. Jalit and G.A. Rivas, *Talanta*, 80 (2010) 2149.
2. H.S. Wang, T.H. Li, W.L. Jia and H.Y. Xu, *Biosens. Bioelectron.,* 22 (2006) 664.
3. H.Y. Wang, Y. Sun and B. Tang. *Talanta,* 57 (2002) 899.
4. H.P. Wu, T.L. Cheng and W.L. Tseng, *Langmuir,* 23 (2007) 7880.
5. V. Carrera, E. Sabater, E. Vilanova, and M.A. Sogorb, *J. Chromatogr. B*, 847(2007) 88.
6. L.L. Li, H.Y. Liu, Y.Y. Shen, J.R. Zhang and J.J. Zhu, *Anal. Chem.,* 83(2011) 661.
7. X.Q. Tian, C.M. Cheng, H.Y. Yuan J. Du, D. Xiao, S.P. Xie and M.M.F. Choi, *Talanta,* 93 (2012) 79.
8. C.X. Xu, K.J. Huang, Y. Fan, Z.W. Wu, J. Li and T. Gan, *Mater. Sci. Engin., C,* 32 (2012) 969.
9. Y.R. Kim, S. Bong, Y.J. Kang, Y. Yang, R.K. Mahajan, J.S. Kim and H. Kim, *Biosens. Bioelectron.,* 25 (2010) 2366.
10. S.R. Hou, N. Zheng, H.Y. Feng, X.J. Li and Z.B. Yuan., *Anal. Biochem.,* 179 (2008) 179.
11. S.C. Fernandes, I.C. Vieira, R.A. Peralta and A. Neves., *Electrochim. Acta,* 55 (2010) 7152.
12. D.P. Quan, D.P. Tuyen, T.D. Lam, P.T.N. Tram, N.H. Binh and P.H. Viet, *Colloids Surf., B:*

Biointerfaces, 88 (2011) 764.
13. T. Thomas, R.J. Mascarenhas, P. Martis, Z. Mekhalif and B.E.K. Swamy, *Mater. Sci. Engin. C,* 33 (2013) 3294.
14. J.B. Zheng and X.L. Zhou. *Bioelectrochem.,* 70 (2007) 408.
15. X. Cao, X.L. Cai and N. Wang. *Sens. Actuators B,* 160 (2011) 771.
16. A.A. Abdelwahab, H.M. Lee and Y.B. Shim. *Anal. Chim. Acta,* 650 (2009) 247.
17. Y.F. Zhao, Y.Q. Gao, D.P. Zhan, H. Liu, Q. Zhao, Y. Kou, Y.H. Shao, M.X. Li, Q.K. Zhuang and Z.W. Zhu, *Talanta,* 66 (2005) 51.
18. Y. Huang, C.M. Cheng, X.Q. Tian, B.Z. Zheng, Y. Li, H.Y. Yuan, D. Xiao and M.M.F. Choi, *Electrochim. Acta,* 89 (2013) 832.
19. S.J. Li, D.H. Deng, Q. Shi and S.R. Liu, *Microchim. Acta,* 177 (2012) 325.
20. B. Kaur, T. Pandiyan, B. Satpati and R. Srivastava, *Colloids Surf., B: Biointerfaces,* 111 (2013) 97.
21. P. He, W. Wang, L.C. Du, F.Q. Dong, Y.Q. Deng and T.H. Zhang, *Anal. Chim. Acta,* 739 (2012) 25.
22. C.L. Sun, H.H. Lee, J.M. Yang and C.C. Wu, *Biosens. Bioelectron.,* 26 (2011) 3450.
23. Y.J. Guo, S.J. Guo, J.T. Ren, Y.M. Zhai, S.J. Dong and E.K. Wang, *ACS Nano,* 4 (2010) 4001.
24. L. Tan, K.G. Zhou, Y.H. Zhang, H.X. Wang, X.D. Wang, Y.F. Guo and H.L. Zhang, *Electrochem. Commun.,* 12 (2010) 557.
25. Q. Liu, X. Zhu, Z.H. Huo, X.L. He, Y. Liang and M.T. Xu, *Talanta,* 97 (2012) 557.
26. N. Lavoie, P.R.L. Malenfant, F.M. Courtel, Y.Abu-Lebdeh and I.J. Davidson, *J. Power Sources,* 213 (2012) 249
27. Y.F. Fan, X.D. Zhang, Y.S. Liu, Q. Cai and J.M. Zhang, *Mater. Lett.,* 95 (2013) 153.
28. Y.Z. Wu, S.Q. Liu, H.Y. Wang, X.W. Wang, X. Zhang and G.H. Jin, *Electrochim. Acta*, 90 (2013) 210.
29. N. Li, Z.F. Geng, M.H. Cao, L. Ren, X.Y. Zhao, B. Liu, Y. Tian and C.W. Hu, *Carbon*, 54 (2013) 124.
30. A. Salimi, K. Abdi and G.R. Khayatian. *Microchim. Acta,* 144 (2004) 161.
31. H. Bai, Y.X. Xu, L. Zhao, C. Li and G.Q. Shi, *Electrochem. Commun.*, 13 (2009) 1667.
32. F. Wu, H.W. Lin, X. Yang and D.Z. Chen, *Int. J. Electrochem. Sci.,* 8 (2013) 7702.
33. X. Yang, F. Wu, D.Z. Chen and H.W. Lin, *Sens. Actuators. B,* 192 (2014) 529.
34. X.Yang, F. Zhang, Y.J. Hu, D.Z. Chen, Z.Q He and L.Z. Xiong, *Int. J. Electrochem. Sci.,* 9 (2014) 5061.
35. A.H. Liu, M.D. Wei, I. Honma and H.S. Zhou, *Adv. Funct. Mater.* 16 (2006) 371.
36. Y. Tong, Z.C. Li, X.F. Lu, L. Yang, W.N. Sun, G.D. Nie, Z.J. Wang and C. Wang, *Electrochim. Acta,* 95 (2013) 12.
37. X. Yang, F.B. Xiao, H.W. Lin, F. Wu, D.Z. Chen and Z.Y. Wu, *Electrochim. Acta,* 109 (2013) 750.
38. J. Li, J. Yang, Z.J. Yang, Y.F. Li, S.H. Yu, Q. Xu and X.Y. Hu., *Anal. Methods,* 4 (2012) 1725.
39. A.S. Adekunle, B.O. Agboola, J. Pillay and K.I Ozoemena., *Sens. Actuators, B,* 148 (2010) 93.